J. Eng. Technol. Sci., Vol. 53, No. 4, 2021, 210409

Free Convection of Ag/H_2O Nanofluid in Square Cavity with Different Position and Orientation of Egg Shaped Cylinder

Hayder K. Rashid[1], Mushtaq F. Almensoury[2], Atheer Saad Hashim[3,*], Hameed K. Hamzah[4] & Farooq H. Ali[4]

[1]College of Material Engineering, Ceramic Engineering Department, University of Babylon, Babylon, Iraq.
[2]Mechanical Engineering Department, College of Engineering, University of Al-Qadisiyah, Diwaniyah, Iraq
[3]Water Resources Engineering College, Al-Qasim Green University, Iraq
[4]Mechanical Engineering Department, College of Engineering, University of Babylon, Babylon, Iraq
*E-mail: atheersaadhashim@wrec.uoqasim.edu.iq

Highlights:

- The Nusselt number location around the egg shaped cylinder curve is affected by the position and inclination angle of the cylinder.
- The optimal position for the cylinder is when it is close to the upper wall and its pointed end is to the left.
- The natural heat convection by an egg shaped cylinder can be enhanced by increasing the Rayleigh number.

Abstract: A numerical simulation was conducted to study the free convection of Ag/H_2O nanofluid between a square cavity with cold walls and an egg shaped cylinder with a hot wall. Utilizing the egg equation, dimensionless governing equations were solved using the Galerkin Finite Element Method (GFEM). In this work, several parameters were studied, i.e. Rayleigh number ($10^3 \leq Ra \leq 10^6$), volume fraction ($0 \leq \varphi \leq 0.05$), position ($-0.2 \leq Y \leq 0.2$), and orientation angle ($-90° \leq \gamma \leq 90°$). The numerical results are presented as streamline contours, isotherm contours, and local and average Nusselt numbers. Moreover, the results were used to analyze the fluids' structure, temperature distribution, and heat transfer rate. The numerical results confirmed that the stream intensity value increased with an increase of the Rayleigh number as well as the movement of the cylinder towards the bottom wall for all values of the orientation angle. Variation of the vertical position of the cylinder inside the cavity had a noticeable effect on Nu_L, which increased by 50% at γ = -90°, and by 58% at γ = -45°. However, at Y = -0.2, Nu_L increased by 58% at γ = -45° and decreased by 7% at γ = -90°. The highest heat transfer rate was obtained at high Rayleigh number ($Ra = 10^6$), volume fraction (φ = 0.05), negative position (Y = -0.2), and the highest positive orientation angle (γ = 90°).

Received March 21st, 2020, 1st Revision November 17th, 2020, 2nd Revision January 31st, 2021, Accepted for publication May 30th, 2021.
 ISSN: 2337-5779, DOI: 10.5614/j.eng.technol.sci.2021.53.4.9

Keywords: *egg shaped cylinder; GFEM; natural convection; nanofluids; square cavity.*

1 Introduction

Natural convection is a common heat transfer mechanism in many everyday physical applications. The natural convection process inside an enclosure has received attention from many researchers due to its wide range of applications, for example in heat exchangers, cooling systems of electronics parts, collectors of solar energy systems, oil storage tanks, and the boundary layer of the stratified atmosphere [1,2]. In order to increase efficiency, researchers have developed different methods to enhance the natural convection processes by choosing the envelope shape and by changing the physical and thermal properties of the working fluid [3-9]. For example, researchers have added nano-magnetic particles at different volume fractions to change the thermodynamic behavior of the fluid [10-12]. Haddad, *et al.* [13] presented a very good review of using nanofluids as working fluid for heat transfer by natural convection. They concluded that the use of a nanofluid is suitable for natural convection and other heat transfer processes due to the enhancement of the thermal properties of the nanofluid. In addition, changing the shape of the enclosure is another way of enhancing the natural convection process that has been studied by researchers [13]. Some of them preferred using a triangular enclosure [14,15] of different dimensions or a rectangular shape with different side dimensions [16-19]. For example, Aminossadati & Ghasemi [16] studied the natural convection heat transfer processes inside an enclosure using a nanofluid as working fluid in the presence of a heat source. They concluded that cooling performance increased with increasing volume fraction of the nanoparticles, especially at low Rayleigh numbers. Other researchers have presented non-uniform shapes such as a semi-annulus trapezoidal configuration [20], complex C-shapes [21-26], annulus and semi-annulus shapes [22,23], and an F-shape [27].

To understand how the shape of the enclosure affects the natural convection heat transfer processes, some important studies are reviewed and presented in this paper. For example, Ahmed, *et al.* [26] studied the natural convection through a rectangular channel using nonlocal mathematical models and Robin boundary conditions. A nanofluid was used as the working fluid to enhance the heat transfer processes. They concluded that the convection processes could be enhanced with the presence of a nanofluid and could be increased by increasing the nanoparticle volume fraction. Convection heat transfer inside a C-shaped enclosure due to a heat source was studied by Mohebbi [28]. The Boltzmann method was used to solve the mathematical model. A nanofluid was used as working fluid and similar results about enhancing the convection heat transfer process were found. The Nusselt number for different values of Reynolds number, streamlines, and isotherms were presented by Ma, *et al.* [29,30].

Mahmoudi, *et al.* [31] studied the heat transfer by natural convection inside a triangular enclosure. They assumed that the temperature of the vertical and inclined walls were low when a heat source was applied to the bottom wall of the enclosure. They showed that the entropy generation and Nusselt number decreased with the increasing nanoparticle volume fraction of specific Reynolds numbers. In Abu-Nada, *et al.* [23] natural convection between two concentric annuli was studied using different types of nanofluids. They showed that the heat transfer processes could be enhanced by increasing the volume fraction and using a magnetic particle of higher thermal conductivity at higher values of the Reynolds number. The reverse effect was shown at lower values of the Reynolds number. The convection heat transfer process between elliptical and cylindrical cylinders was studied by Seikholeslami, *et al.* [32]. A nanofluid was considered as working fluid inside an enclosure. They found that the Nusselt number increased with increasing volume fraction and Rayleigh number. Tayebi & Chamkha [33] investigated the natural convection in an enclosure created by two confocal-elliptical cylinders using hybrid fluids: Cu-Al2O3/water and Al2O3/water. They generally concluded that a better heat transfer process was achieved with the first hybrid nanofluid than with the second nanofluid. Matin & Pop [34] studied heat transfer and fluid flow between two concentric annuli. The study was carried out by numerical simulation in conjunction with the formulation of a stream function and vortices in a polar coordinate representation. The results showed that an increasing volume fraction of the nanoparticles led to an increase in the Nusselt number inside the enclosure.

Hatami & Safari [35] studied the heat transfer process for a heated cylinder inside an enclosure with a wavy wall. They intended to find the optimum location of the cylinder inside the enclosure. They explained that applying heat to central locations of the cylinder was the best method for improving the heat transfer performance. Natural convection inside an enclosure created by a horizontal cylinder inside a square cavity was presented by Sheikholeslami, *et al.* [36]. The enclosure was filled with a nanofluid and a magnetic field was considered to be present. The inner cylinder was assumed to have a higher temperature than the outer cylinder. They showed that a higher Nusselt number can be obtained by increasing the volume fraction of the nanoparticles. Yuan, *et al.* [37] studied the effect of enclosure geometry on the natural convection process. Three shapes were studied: cylindrical, square, elliptical, and triangular. They explain that a considerable change in the heat transfer can be achieved by changing the enclosure geometry. Ali, *et al.* [38-39] investigated the effect of a sinusoidal wall on natural convection in two articles. The first one studied the natural convection inside a square enclosure with two sinusoidal vertical walls. The second one involved natural convection inside a square enclosure with one wall that is a sinusoidal and circular hot inner cylinder. Hamzah, *et al.* [40-41] studied a free convection trapezoid and square, respectively, filled with Cu/H_2O nanofluid with

different boundary conditions. The results showed that added nanoparticles enhanced the heat transfer rate.

There are limited research studies about a hot object within a cold-wall square enclosure. This principle of cold walls around hot inner bodes can be utilized to extend the thermal life of electrical and electronic equipment. Other applications can be found in nuclear reactors, automobiles, computers, air conditioning, aeronautics, maritime transportation, solar and geothermal energy, terrestrial apparatus, and the food, agricultural and pharmaceutical industries.

After studying the literature on these topics, we note that free convection heat transfer produced through the space between a hot surface located in a cavity has received great interest, as it is basic to a wide range of engineering and industrial applications. Common shapes inside a square enclosure have been considered, for example circles, squares, triangles, and rectangles. The objective of the present work was to find the maximum and minimum heat transfer rate with an unfamiliar shape (egg shaped cylinder) in different positions and with different orientations inside a square enclosure. This shape can be used to control the heat transfer inside the square enclosure by changing its location and orientation. The reason behind the use of Ag nanoparticles was that they have great interest due to their extensive use in chemical and biomedical applications, bags for food storage, refrigerator surfaces, personalized care products, etc. Silver nanoparticles have special physical characteristics in size and shape, as they are small and have a high specific area (ratio between surface area and mass) and high thermal conductivity. Therefore they have high re-action and anti-bacterial action.

2 Physical Model Characterization

A two-dimensional square cavity was utilized with length and height equal to the unity length (H) and with an egg shaped cylinder with base radius equal to (0.2H), as depicted in Figure 1. All cavity walls were cold (T_c), whereas the egg shaped cylinder wall was hot (T_h). The egg function in Eq. (1), generalized in Equation (2), was introduced to study the natural convection inside the cavity filled with a silver-water nanofluid. Steady, incompressible, laminar natural convection was considered in the present work. The studied variables were Rayleigh number $10^3 \leq Ra \leq 10^6$, volume fraction $0 \leq \varphi \leq 0.06$, vertical location $-0.2 \leq Y_o \leq 0.2$, and orientation $-90° \leq \gamma \leq 90°$. The thermo-physical properties of the base fluid (water) and nanoparticles (silver) were assumed to be in a state of thermal equilibrium and tilted, as presented in Table 1. Also, the heat capacity and thermal conductivity were assumed to be unchanging, while the density changed according to the Boussinesq approximation due to the temperature difference.

$$x^2 + y^2 * [1.6 * 1.4^x]^2 = 1 \quad (1)$$

$$X^2 + Y^2 * [1.6 * 1.4^X]^2 = R^2 \quad (2)$$

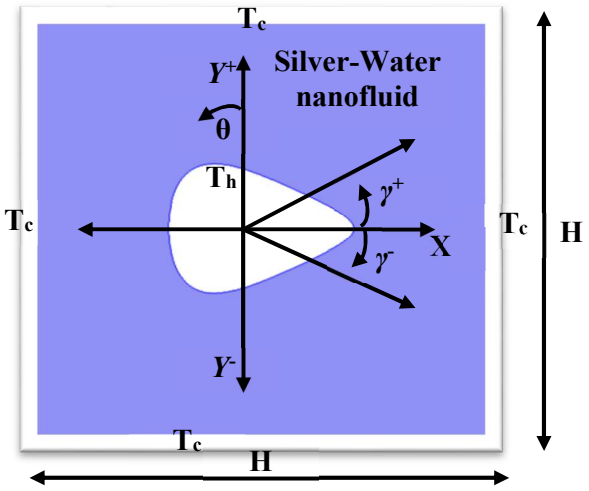

Figure 1 Simplified diagram of physical principle of the present study.

3 Governing Equations and Boundary Conditions

The governing equations of continuity, momentum, and energy for 2-dimensional, steady-state, laminar natural convection in the absence of dissipation of viscosity, generation of heat, and heat radiation can be written as follows [15,18-20]:

$$\frac{\partial u}{\partial x} + \frac{\partial v}{\partial y} = 0 \quad (3)$$

$$u\frac{\partial u}{\partial x} + v\frac{\partial u}{\partial y} = -\frac{1}{\rho_{na}}\frac{\partial p}{\partial x} + \frac{\mu_{na}}{\rho_{na}}\left(\frac{\partial^2 u}{\partial x^2} + \frac{\partial^2 u}{\partial y^2}\right) \quad (4)$$

$$u\frac{\partial v}{\partial x} + v\frac{\partial v}{\partial y} = -\frac{1}{\rho_{na}}\frac{\partial p}{\partial y} + \frac{\mu_{na}}{\rho_{na}}\left(\frac{\partial^2 v}{\partial x^2} + \frac{\partial^2 v}{\partial y^2}\right) + g\beta_{na}(T - T_c) \quad (5)$$

$$u\frac{\partial T}{\partial x} + v\frac{\partial T}{\partial y} = \alpha_{na}\left(\frac{\partial^2 T}{\partial x^2} + \frac{\partial^2 T}{\partial y^2}\right) \quad (6)$$

where u and v are the x-velocity and y-velocity respectively, T is the temperature of the fluid, p is the pressure, g is the gravity due to acceleration. Other physical properties are defined in the nomenclature. 'T_o' converts the governing equation from dimensional form to non-dimensional form. The following non-dimensional parameters are indicated:

$$X,Y = \frac{x,\ y}{H}\ , U,V = \frac{(u,v)*H}{\alpha_{bf}}, P = \frac{pH^2}{\rho_{na}\alpha_{bf}^2}, T^* = \frac{T-T_c}{T_h-T_c} \tag{7}$$

After applying the above non-dimensional parameters in Eq. (7), Eqs. (3)-(6) can be changed to non-dimensional form as follows:

$$\frac{\partial U}{\partial X} + \frac{\partial V}{\partial Y} = 0 \tag{8}$$

$$U\frac{\partial U}{\partial X} + V\frac{\partial U}{\partial Y} = -\frac{\partial P}{\partial X} + \frac{\mu_{na}}{\rho_{na}\alpha_{bf}}\left(\frac{\partial^2 U}{\partial X^2} + \frac{\partial^2 U}{\partial Y^2}\right) \tag{9}$$

$$U\frac{\partial V}{\partial x} + V\frac{\partial V}{\partial y} = -\frac{\partial P}{\partial Y} + \frac{\mu_{na}}{\rho_{na}\alpha_{bf}}\left(\frac{\partial^2 V}{\partial X^2} + \frac{\partial^2 V}{\partial Y^2}\right) + RaPrT^* \tag{10}$$

$$U\frac{\partial T^*}{\partial X} + V\frac{\partial T^*}{\partial Y} = \frac{\alpha_{na}}{\alpha_{bf}}\left(\frac{\partial^2 T^*}{\partial X^2} + \frac{\partial^2 T^*}{\partial Y^2}\right) \tag{11}$$

The non-dimensional numbers Pr and Ra are given as:

$$Pr = \frac{\nu_{bf}}{\alpha_{bf}}, Ra = \frac{g\beta(T_h - T_c)H^3}{\alpha_{bf}\nu_{bf}}$$

The silver/water nanofluid properties are expressed by the following relations [10,11,14-16]:

Nanofluid density is defined as

$$\rho_{na} = (1-\varphi)\rho_{bf} + \varphi\rho_{sp} \tag{12}$$

where ρ_{bf} and ρ_{sp} are the density of the base fluid and solid nanoparticles.

The nanofluid volumetric expansion coefficient is expressed as

$$(\rho\beta)_{na} = (1-\varphi)(\rho\beta)_{bf} + \varphi(\rho\beta)_{sp} \tag{13}$$

The nanofluid heat capacity is expressed by

$$(\rho c_p)_{na} = (1-\varphi)(\rho c_p)_{bf} + \varphi(\rho c_p)_{sp} \tag{14}$$

The nanofluid thermal conductivity is defined by using the Maxwell model [42]. This model has been used by extensively researchers, for example as

$$\frac{k_{na}}{k_{bf}} = \left[\frac{(k_{sp}+2k_{bf})-2\varphi(k_{bf}-k_{sp})}{(k_{sp}+k_{bf})+\varphi(k_{bf}-k_{sp})}\right] \tag{15}$$

The nanofluid dynamic viscosity is expressed by using the Brinkman model [42] as follows

$$\mu_{na} = \frac{\mu_{bf}}{(1-\varphi)^{2.5}} \tag{16}$$

The flow structure in the inner region of the cavity is explained by means of streamlines, where the streamlines are derived from velocity components U and V. The equations related to the velocity components and streamlines for 2D study are:

$$U = \frac{\partial \Psi}{\partial Y}, V = -\frac{\partial \Psi}{\partial X} and \ \frac{\partial^2 \Psi}{\partial X^2} + \frac{\partial^2 \Psi}{\partial Y^2} = \frac{\partial U}{\partial Y} - \frac{\partial V}{\partial X} \tag{17}$$

The heat transfer rate is described by the local and average Nusselt number, which are considered from the following two equations [32]:

$$Nu_L = \frac{\partial T^*}{\partial n} \tag{18}$$

$$Nu_{ave} = \frac{1}{2\pi}\int_0^{2\pi} Nu_L(\theta) d\theta \tag{19}$$

Thermo-physical properties of the silver/water nanofluid are tabulated in Table 1.

The boundary conditions of the present study were defined as follows:

1. Outer cavity walls: U = V = Ψ = 0, T* = 0
2. Inner egg shaped cylinder: U = V = Ψ = 0, T* = 1

4 Numerical Formulation and Code Validation

The non-dimensional governing Eqs. (8-11) with corresponding boundary conditions were solved numerically by using the finite element method built on Galerkin's weighted residual formulation in COMSOL Multiphysics. The independency mesh test of the laminar natural convection done in this study is listed in Table 2, which describes the mesh accuracy of a coarse mesh (M1) to an extremely fine mesh (M7) in the first column. The second and third columns contain the domain and boundary element. The fourth column contains the time elapsed to obtain the convergent solution. The fifth column contains the average Nusselt number of the egg shaped cylinder. The average Nusselt number was taken as reference parameter because it was represented as a global parameter in this study. The error in the Nusselt number is shown in the sixth column. The percentage error was 0.0001%, which can be seen as insignificant. Triangular elements were used for the mesh, as described in Figure 2.

To check the code credibility, a comparison was made with the results published by Basak & Chamkha [42] of the average Nusselt number, as shown in Table 3, for different Rayleigh numbers and volume fractions as well as for the isotherms and streamline contours in Figure 2. The comparison showed excellent agreement for all studied variables, i.e. heat transfer rate, temperature distribution, and fluid flow pattern.

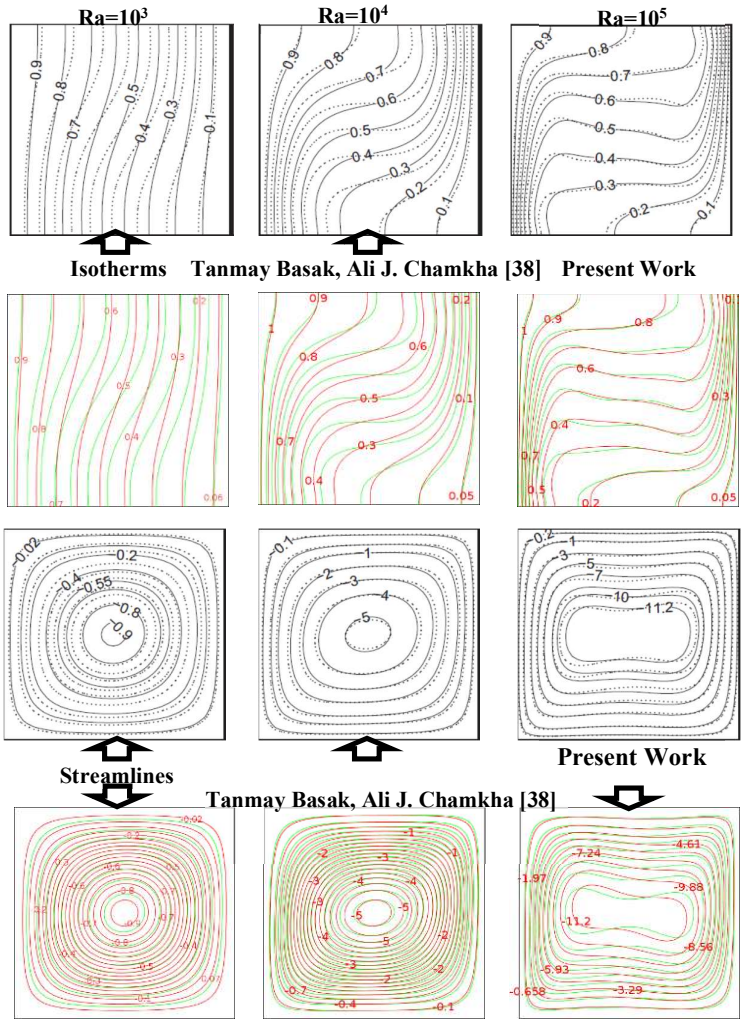

Figure 2 Similarity between isotherms and streamlines between Basak & Chamkha [38] and the present work.

5 Results and Discussion

There are many different geometrical heating shapes and inclination angles that can be applied in the application of an enclosure. The working fluid and nanofluid particle properties are very important in restricting the convection flow. The intrinsic evolution of the simulation of an innovative shape (a hot egg shaped cylinder) surrounded by a nanofluid inside a cold-wall square enclosure was

studied. The egg shaped cylinder affects the flow and influences the heat transfer rate, a fact that can be used in many applications to control the heat transfer rate. The free convection mechanism inside a square cavity is explained briefly in the following part. The nanoparticles of the working fluid that are close to the hot walls gain heat earlier than particles that are far from the wall. This conduction results in variations in the temperature of the nanofluid. Thus, the heat expands the fluid and causes a change in the density of the heated part, which consequently leads to density differences in the working fluid. This induces flow by buoyancy forces. The nanofluid rises upward and cools until it reaches the cold wall, where the heat has almost completely been dissipated from the hot nanofluid. Thus, its density increases. The denser nanofluid becomes cool and heavy, going down under the effect of the gravitational force. Closer to the hot egg cylinder, the cold nanofluid gradually warms up again, so a circulation pattern occurs. This continues as long as there is a reasonable temperature gradient.

Figure 3 shows the streamlines and isotherms for different positions and inclination angles of the egg shaped cylinder for Ra = 10^4. This figure shows positions of the egg shaped cylinder on the Y-axis (Y) in the columns and the orientation/inclination angle 0° of the egg cylinder in the rows. The figure shows that the change of the inclination angle for $Y = 0$ has less distortion than in other positions, where the heat transfer rate is improved in comparison with other angles of the egg shaped cylinder in this position. The thermal distribution from the hot cylinder to the cold-wall cavity is semi-uniform, whereas in the other positions ($Y = \pm 0.2$), the distribution is non-uniform due to the egg shaped cylinder being closer to one wall than the other. On the other hand, for the streamline function, two semi-symmetrical opposite flow direction vortices can be observed on the left and the right with the hot egg shaped cylinder at $Y = 0.2$ or $Y = -0.2$. In addition, the thermal lines have a uniform distribution around the hot egg shaped form for all results except $\gamma = \pm 90°$ at Y = 0, as it is uniform and symmetric about the Y-axis. Moreover, the thermal lines have been disturbed adjacent to the pointed end of the egg shaped cylinder, which is very clear at an angle of $\gamma = -45°$ with Y = 0.2, which resulted from the role of the cylinder's pointed end in struggling with the flow and could lead to accumulation of the temperature gradient. Besides, the maximum effect of natural convection on the streamline function values can be seen for the same position at $Y = 0.2$ with $\gamma = 0°$. A possible explanation is the physical fact that in the heat transfer between two parallel surfaces, the heat is transmitted by convection when the lower surface is hot and the upper one is cold due to the influence of the difference in density (buoyancy force). It is transferred by conduction when the upper surface is hot and the lower surface is cold. Thus, with regard to the egg shaped cylinder, whenever it is located close to the cavity's bottom, the greater the area of the curve of the cylinder, the greater the flow path and, consequently, the greater the obstruction of flow in adjacent areas. This leads to forming relatively stagnating

areas, which could make the heat transfer become dominated by conduction, which has a better heat transfer rate than convection [43].

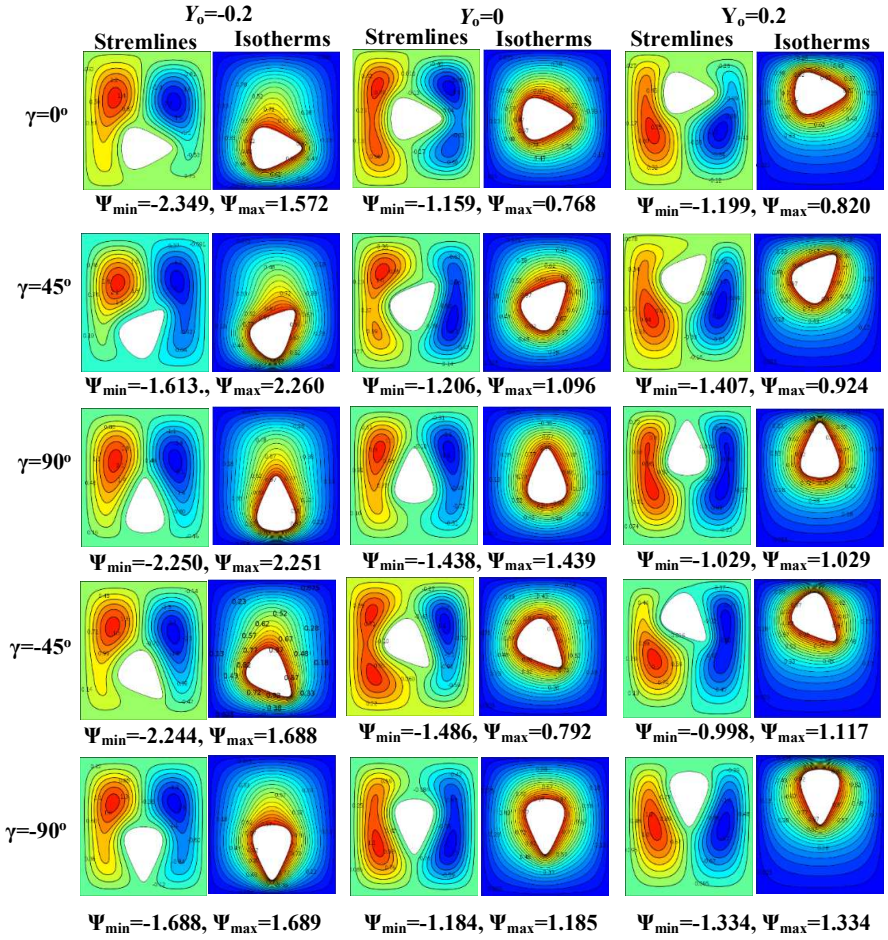

Figure 3 Streamlines, isotherms for different positions and inclination angles for Ra = 10^4.

In general, when compared to outcomes for Ra = 10^4, Figure 4 shows a similar behavior of the streamlines and isotherms at Ra = 10^6. However, it exhibits higher values and an exaggerated deformation in the thermal lines and flows as the convection rate increases and the Rayleigh number increases. In particular, small vortices in the flow appear noticeably at the wider end of the cylinder for $Y = 0.2$ with γ = -90°. As can be seen in this figure, the results associated with the streamlines and isotherms for different positions and the heat transfer

enhancements are very clear, where the geometry shape and its position have a significant interplay effect on the flow pattern. For $Y = 0.2$ and for all orientation angles, the pointed end of the egg shaped cylinder enhanced the heat transfer rate.

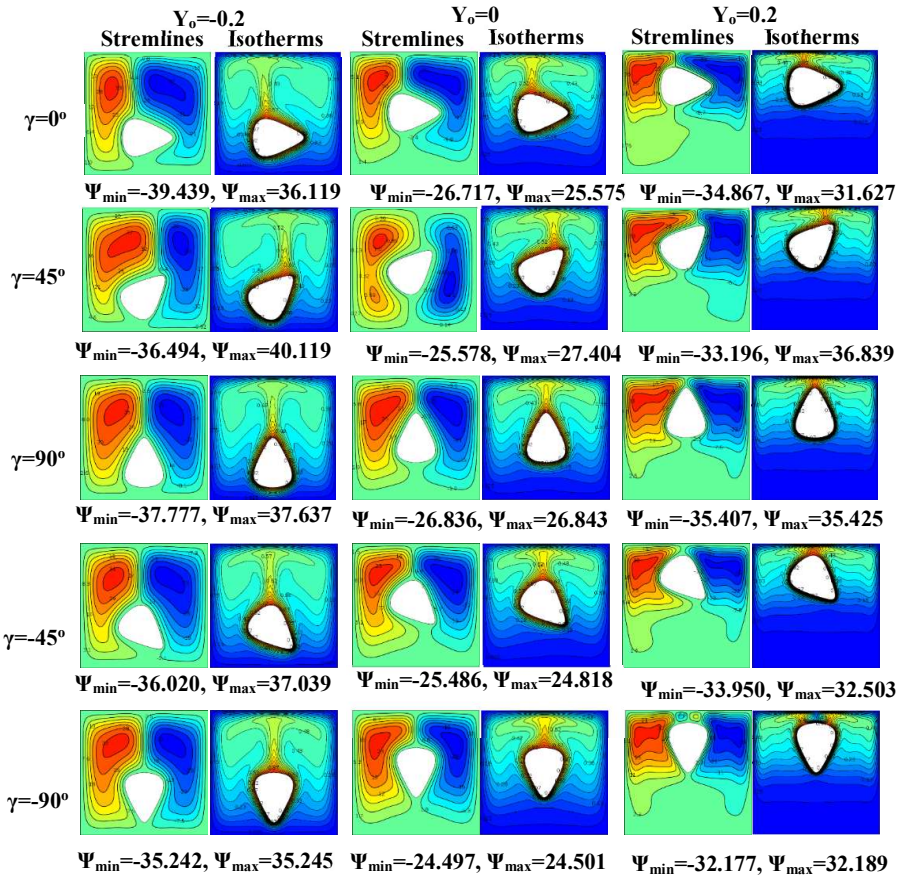

Figure 4 Streamlines, isotherms for different positions and inclination angles for $Ra = 10^6$.

Thus, a turbulent flow was induced at this part of the cylinder. For this reason it is necessary to investigate the local Nusselt number around the boundary locations of the egg shaped cylinder for $Ra = 10^6$ for all inclination angles to depict its influence on the effectiveness of the heat transfer. In addition, the values of the streamlines and isotherms were very high compared with the results for $Ra = 10^4$. However, confusion occurs in the isotherm contours throughout the enclosure and more densely in the vicinity of the hot egg shaped cylinder for all

locations and inclination angles. In addition, the impact of the cylinder on the isotherms in downward positions is visible in this region for all rotation angles. In contrast, the impact on the isotherm was stronger closer to the upper region of the cavity for Y = 0.2 and all inclination angles. The Nu_L around the hot egg shaped cylinder for different positions and inclination angles and Ra = 10^6, φ = 0.05 can be seen in Figure 5.

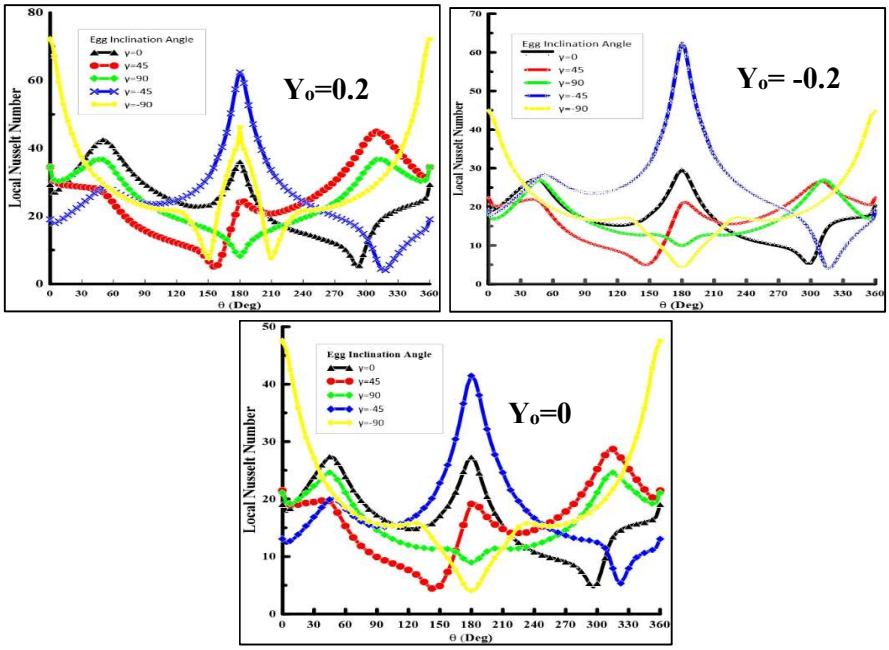

Figure 5 Local Nusselt number around hot egg shaped cylinder for different positions and inclination angles for Ra = 10^6, φ = 0.05.

However, Figure 5 shows that at γ = -45° convection was better at θ = 0° and 360° (pointed end) due to the flow becoming turbulent. This results from the non-uniform shape of the cylinder, which makes free convection at the right part of the pointed tip occur earlier than on the left, in addition to the noticeable velocity difference on both sides of the egg shaped cylinder. In contrast, far from the top of the egg shaped cylinder (θ = 0°, 360° or ±45°), the flow stays laminar and the obstruction by the cylinder's boundary has only a marginal effect.

Firstly, in position of Y = 0 at angle γ = -90°, the height Nu_L was 48 at $\theta = 0$, but it reached its minimum value ($Nu_L = 4$) at $\theta = 180^o$. Regarding $\gamma = -45^o$, Nu_L = 13 at $\theta = 0$, but it reached its maximum level ($Nu_L = 44$) at $\theta = 180^o$.

Secondly, for Y = 0.2 and γ = -90°, Nu_L is 72 at $\theta = 0$, but it reached its minimum value ($Nu_L = 8$) at $\theta = 150^o$ and 210^o. With regard to $\gamma = -45^o$, Nu_L = 20 at $\theta = 0$, but it reached its maximum level ($Nu_L = 63$) at $\theta = 180^o$. Finally, for Y = -0.2 and γ = -90°, Nu_L is 45 at $\theta = 0$, but it reached its minimum value ($Nu_L = 3$) at $\theta = 180^o$. Regarding $\gamma = -45^o$, Nu_L = 18 at $\theta = 0$, however, it reached its maximum level ($Nu_L = 64$) at $\theta = 180^o$.

Furthermore, the situations at γ = -90° and γ = 90° had a counteractive effect compared with other rotation angles in most of the cases in the simulation, because the strength of the natural convection at γ = -90° and γ = 90° dropped by keeping the flow laminar in almost the whole cavity. For = -90° for Y = 0.2, the Nusselt number was higher due to the increased natural convection caused by the turbulent flow adhering to the middle of the cylinder's surface. Figure 6 shows the relation between the average Nusselt number and the Rayleigh number around the hot egg shaped cylinder for different values of Y_o and γ at φ = 0.05. From this figure, the effect of the Rayleigh number on the average Nusselt number for Ra = 10^6 can be seen.

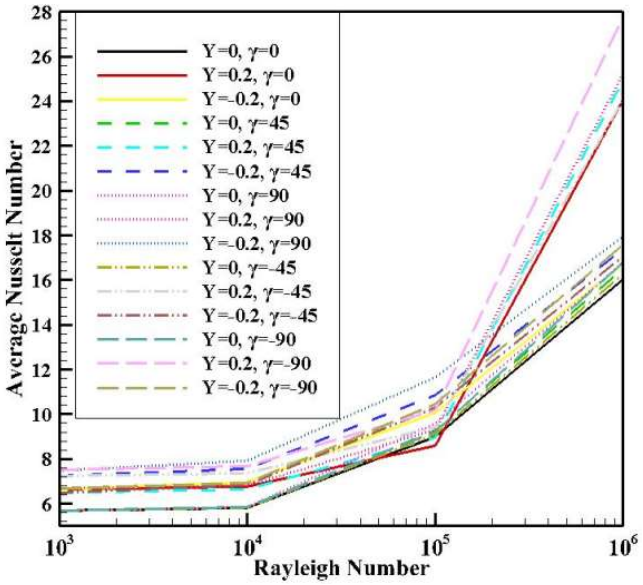

Figure 6 The average Nusselt number and the Rayleigh number around the hot egg shaped cylinder for different vaues of Y_o and γ at φ = 0.05.

Where there were sudden changes in Nusselt values for Y = 0.2 for all values of the orientation angle (γ), Figure 7 reveals the direct relationship between the

average Nusselt number and the volume fraction (φ) around the hot egg shaped cylinder for different Rayleigh numbers ($Y_o = 0$, $\gamma = 0°$). The relationship proves that Nu increases as Ra increases, which adds to the increase in volume fraction, leading to further improvement of the heat transfer rate. This explains the important role of the nanofluid in thermal enhancement. This means that additive Ag nanoparticles enhance the heat transfer rate compared to using a pure fluid. Also, this improvement increases with increasing Rayleigh number, since the silver particles then become more active.

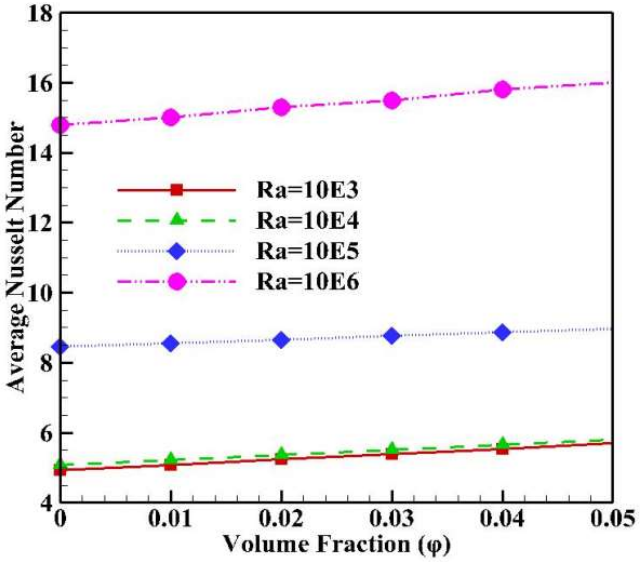

Figure 7 The average Nusselt number and volume fraction around the hot egg shaped cylinder for different Rayleigh numbers and $Y_o = 0$, $\gamma = 0°$.

6 Conclusion

In this study, the effect of a special hot egg shaped cylinder inserted in a cold square shaped cavity containing a silver-water nanofluid on the heat transfer rate was numerically computed for various positions and rotating angles of the cylinder. The influence of Rayleigh number and volume fraction were investigated. The conclusions can be summarized as follows:

1. The position of the hot egg shaped cylinder has a great influence on the heat transfer rate and the best position is at $Y = 0.2$.
2. Increasing the Rayleigh number induces a perfect situation by increasing the strength of natural convection, which helps to observe the hot egg shaped

cylinder's effect on isotherm confusion, the streamline values and distribution type.

3. Changing the rotation angles of the hot egg cylinder from zero ($\gamma \neq 0$) within the cold square shaped cavity enhanced the heat transfer rate especially at γ = -45°.
4. The effect of changes in the cylinder's location on the Y axis was clear. At Y above zero, at $\theta = 0^{o}$, the change rate of Nu_L increased at γ = -45° and γ = -90°, by 58% and 50% respectively. At Y below zero, Nu_L increased by 58% at γ = -45° , but it decreased by 7% at γ = -90°.
5. The best conditions for using the egg shaped cylinder in producing a turbulent flow and enhancing the heat transfer rate are Y = 0.2 and Ra = 10^6.
6. The variation of volume fraction in the case under investigation showed a flagged effect compared with other parameters, especially the Rayleigh number.

The Nusselt number at the pointed end (small radius) of the egg cylinder is greater than the Nusselt number in a convex region (large radius) in almost all situations.

Nomenclature

Roman letters

C_p = *Specific heat at constant pressure (KJ/kg.K)*
G = *Gravitational acceleration (m/s^2)*
K = *Thermal conductivity (W/m.K)*
H = *Length and height of cavity*
R = *Dimensionless radius of egg cylinder shape*
R = *Radius of egg cylinder shape (m)*
P = *Dimensionless pressure*
P = *Pressure (Pa)*
Pr = *Prandtl number (ν_f/α_f)*
Ra = *Rayleigh number* $(g\beta_{bf}L^3\,\Delta T/\nu_{bf}\alpha_{bf})$
T = *Temperature (K)*
T_c = *Temperature of the cold surface (K)*
T_h = *Temperature of the hot surface (K)*
T^* = *Dimensionless temperature*
Nu_L = *Local Nusselt number on the hot inner cylinder*
Nu_{ave} = *Average Nusselt number around egg cylinder*
U = *Dimensionless velocity component in x-direction*
u = *Velocity component in x-direction (m/s)*
V = *Dimensionless velocity component in y-direction*
v = *Velocity component in y-direction (m/s)*
X = *Dimensionless coordinate in horizontal direction*

x	=	*Cartesian coordinates in horizontal direction (m)*
Y, Y_o	=	*Dimensionless coordinate in vertical direction*
y	=	*Cartesian coordinate in vertical direction (m)*
Gr	=	*Grashof number*
Y_o	=	*Position of egg cylinder*
α	=	*Thermal diffusivity (m^2/s)*
θ	=	*Angle of egg cylinder*
Ψ	=	*Dimensional stream function (m^2/s)*
ψ	=	*Dimensionless stream function*
φ	=	*Volume fraction percentage*
γ	=	*Orientation angle*
μ	=	*Dynamic viscosity (kg.s/m)*
ν	=	*Kinematic viscosity (μ/ρ)(Pa.s)*
β	=	*Volumetric coefficient of thermal expansion (K^{-1})*
ρ	=	*Density (kg/m^3)*
c	=	*Cold*
bf	=	*Base fluid (pure)*
sp	=	*Solid particles*
h	=	*Hot*
na	=	*Nanofluid*

References

[1] Park, S.H., Seo, Y.M., Ha, M.Y. & Park, Y.G., *Natural Convection in a Square Enclosure with Different Positions and Inclination Angles of an Elliptical Cylinder, Part I: A Vertical Array of One Elliptical Cylinder and One Circular Cylinder*, Int. J. Heat Mass Transf., **126**, pp. 173-183, 2018. DOI: 10.1016/j.ijheatmasstransfer.2018.06.034.

[2] Hussain, S.H. & Hussein, A.K., *Numerical Investigation of Natural Convection Phenomena in a Uniformly Heated Circular Cylinder Immersed in Square Enclosure Filled with Air at Different Vertical Locations*, Int. Commun. Heat Mass Transf., **37**(8), pp. 1115-1126, 2010. DOI: 10.1016/j.icheatmasstransfer.2010.05.016.

[3] Acharya, N., Bag, R. & Kundu, P.K., *Influence of Hall Current on Radiative Nanofluid Flow over a Spinning Disk: A Hybrid Approach*, Phys. E Low-Dimensional Syst. Nanostructures, **111**, pp. 103-112, 2019. DOI: 10.1016/j.physe.2019.03.006.

[4] Acharya, N., Das, K. & Kumar Kundu, P., *Ramification of Variable Thickness on MHD Tio2 and Ag Nanofluid Flow over a Slendering Stretching Sheet Using NDM*, Eur. Phys. J. Plus, **131**(9), pp. 303, 2016, DOI: 10.1140/epjp/i2016-16303-4.

[5] Acharya, N., *On the Flow Patterns and Thermal Behaviour of Hybrid Nanofluid Flow Inside a Microchannel in Presence of Radiative Solar*

Energy, J. Therm. Anal. Calorim., **141**(4), pp. 1425-1442, 2020. DOI: 10.1007/s10973-019-09111-w.

[6] Acharya, N., Framing the Impacts of Highly Oscillating Magnetic Field on the Ferrofluid Flow over a Spinning Disk Considering Nanoparticle Diameter and Solid-Liquid Interfacial Layer, J. Heat Transfer, **142**(10), 102503, 2020. DOI: 10.1115/1.4047503.

[7] Acharya, N. & Mabood, F., *On the Hydrothermal Features of Radiative Fe3O4-graphene Hybrid Nanofluid Flow over a Slippery Bended Surface with Heat Source/Sink*, J. Therm. Anal. Calorim., **143**(2), pp. 1273-1289, 2021. DOI: 10.1007/s10973-020-09850-1.

[8] Acharya, N., Maity, S. & Kundu, P.K., *Influence of Inclined Magnetic Field on the Flow of Condensed Nanomaterial over a Slippery Surface: the Hybrid Visualization*, Appl. Nanosci., **10**(2), pp. 633-647, 2020. DOI: 10.1007/s13204-019-01123-0.

[9] Acharya, N., Spectral Quasi Linearization Simulation of Radiative Nanofluidic Transport over a Bended Surface Considering the Effects of Multiple Convective Conditions, Eur. J. Mech. B/Fluids, c. 139-154, 2020. DOI: 10.1016/j.euromechflu.2020.06.004.

[10] Xuan, Y. & Li, Q., *Heat Transfer Enhancement of Nanofluids*, Int. J. Heat Fluid Flow, **21**(1), pp.58-64, 2000. DOI: 10.1016/S0142-727X(99)00067-3.

[11] Bayat, J. & Nikseresht, A.H., *Investigation of the Different Base Fluid Effects on the Nanofluids Heat Transfer and Pressure Drop*, Heat Mass Transf., **47**, pp. 1089–10992011. DOI: 10.1007/s00231-011-0773-0.

[12] Hemmat Esfe, M., Saedodin, S. & Mahmoodi, M., Experimental Studies on the Convective Heat Transfer Performance and Thermophysical Properties of MgO-Water Nanofluid under Turbulent Flow, Exp. Therm. Fluid Sci., **52**(1), pp. 68-78, 2014. DOI: 10.1016/j.expthermflusci.2013.08.023.

[13] Haddad, Z., Oztop, H.F., Abu-Nada, E. & Mataoui, A., *A Review on Natural Convective Heat Transfer of Nanofluids*, Renew. Sustain. Energy Rev., **16**(7), pp. 5363-5378, 2012.

[14] Ghasemi, B. & Aminossadati, S.M., *Brownian Motion of Nanoparticles in a Triangular Enclosure with Natural Convection*, Int. J. Therm. Sci., **49**(6), pp. 931-940, 2010.

[15] Aminossadati, S.M. & Ghasemi, B., *Enhanced Natural Convection in an Isosceles Triangular Enclosure Filled with a Nanofluid*, Comput. Math. with Appl., **61**(7), pp. 1739-1753, 2011.

[16] Aminossadati, S.M. & Ghasemi, B., *Natural Convection Cooling of a Localised Heat Source at the Bottom of a Nanofluid-filled Enclosure*, Eur. J. Mech., **28**(5), pp. 630-640, 2009.

[17] Ho, C.J., Liu, W.K., Chang, Y.S. & Lin, C.C., *Natural Convection Heat Transfer of Alumina-Water Nanofluid in Vertical Square Enclosures: An Experimental Study*, Int. J. Therm. Sci., **49**(8), pp. 1345-1353, 2010.

[18] Lai, F.H. & Yang, Y.T., *Lattice Boltzmann Simulation of Natural Convection Heat Transfer of Al2O3/Water Nanofluids in a Square Enclosure*, Int. J. Therm. Sci., **50**(10), pp. 1930-1941, 2011.

[19] Mahmoodi, M., *Numerical Simulation of Free Convection of Nanofluid in a Square Cavity with an Inside Heater*, Int. J. Therm. Sci., **50**(11), pp. 2161-2175, 2011.

[20] Saleh, H., Roslan, R. & Hashim, I., *Natural Convection Heat Transfer in a Nanofluid-Filled Trapezoidal Enclosure*, Int. J. Heat Mass Transf., **54**(1-3), pp. 194-201, 2011.

[21] Mahmoodi, M. & Hashemi, S.M., *Numerical Study of Natural Convection of a Nanofluid in C-Shaped Enclosures*, Int. J. Therm. Sci., **55**, pp. 76-89, 2012. DOI: 10.1016/j.ijthermalsci.2012.01.002.

[22] Soleimani, S., Sheikholeslami, M., Ganji, D.D. & Gorji-Bandpay, M., *Natural Convection Heat Transfer in a Nanofluid Filled Semi-Annulus Enclosure*, Int. Commun. Heat Mass Transf., **39**(4), pp. 565-574, 2012.

[23] Abu-Nada, E*., Effects of Variable Viscosity and Thermal Conductivity of Al2O3-water Nanofluid on Heat Transfer Enhancement in Natural Convection*, Int. J. Heat Fluid Flow, **30**(4), pp. 679-690, 2009.

[24] Mahajan, A. & Sharma, M.K., *Penetrative Convection in Magnetic Nanofluids via Internal Heating*, Phys. Fluids, **29**(3), 34101, 2017.

[25] Mokhtar, N.F.M., Khalid, I.K., Siri, Z., Ibrahim, Z.B. & Gani, S.S.A., *Control Strategy on the Double-Diffusive Convection in a Nanofluid Layer with Internal Heat Generation*, Phys. Fluids, **29**(10), 107105, 2017.

[26] Ahmed, N., Vieru, D., Fetecau, C. & Shah, S.H*., Convective Flows of Generalized Time-nonlocal Nanofluids Through a Vertical Rectangular Channel*, Phys. Fluids, **30**(5), 52002, 2018.

[27] Almensoury, M.F., Hashim, A.S., Hamzah, H.K. & Ali, F.H., *Numerical Investigation of Natural Convection for a non-Newtonian Nanofluid in F-Shaped Porous Cavity*, Heat Transf, 2021.

[28] Mohebbi, R.., Izadi, M. & Chamkha, A.J., *Heat Source Location and Natural Convection in a C-shaped Enclosure Saturated by a Nanofluid*, Phys. Fluids, **29**(12), pp. 122009, 2017.

[29] Ma, Y., Mohebbi, R., Rashidi, M.M. & Yang, Z., *Study of Nanofluid Forced Convection Heat Transfer in a Bent Channel by Means of Lattice Boltzmann Method*, Phys. Fluids, **30**(3), pp. 32001, 2018.

[30] Mahmoudi, A.H., Pop, I. & Shahi, M., *Effect of Magnetic Field on Natural Convection in A Triangular Enclosure Filled with Nanofluid*, Int. J. Therm. Sci., **59**, pp. 126-140, 2012.

[31] Mahmoudi, A.H., Pop, I., Shahi, M. & Talebi, F., *MHD Natural Convection and Entropy Generation in a Trapezoidal Enclosure Using Cu–water Nanofluid*, Comput. Fluids, **72**, pp. 46-62, 2013.

[32] Sheikholeslami, M., Ellahi, R., Hassan, M. & Soleimani, S., *A Study of Natural Convection Heat Transfer in a Nanofluid Filled Enclosure with Elliptic Inner Cylinder*, Int. J. Numer. Methods Heat Fluid Flow, **24**(8), pp. 1906-1927, 2014.

[33] Tayebi, T. & Chamkha, A.J., *Free Convection Enhancement in an Annulus Between Horizontal Confocal Elliptical Cylinders Using Hybrid Nanofluids*, Numer. Heat Transf. Part A Appl., **70**(10), pp. 1141-1156, 2016.

[34] Matin, M.H. & Pop, I., *Natural Convection Flow and Heat Transfer in an Eccentric Annulus Filled by Copper Nanofluid*, Int. J. Heat Mass Transf., **61**, pp. 353-364, 2013.

[35] Hatami, M. & Safari, H., *Effect of Inside Heated Cylinder on the Natural Convection Heat Transfer of Nanofluids in a Wavy-wall Enclosure*, Int. J. Heat Mass Transf., **103**, pp. 1053-1057, 2016.

[36] Sheikholeslami, M., Gorji-Bandpay, M. & Ganji, D.D., *Magnetic Field Effects on Natural Convection around a Horizontal Circular Cylinder Inside a Square Enclosure Filled with Nanofluid*, Int. Commun. Heat Mass Transf., **39**(7), pp. 978-986, 2012.

[37] Yuan, X., Tavakkoli, F. & Vafai, K., *Analysis of Natural Convection in Horizontal Concentric Annuli of Varying Inner Shape*, Numer. Heat Transf. Part A Appl., **68**(11), pp. 1155-1174, 2015.

[38] Hussain, S.H., Sabah, R. & Hassan Ali, F., *Numerical Study of Natural Convection Heat Transfer of Air Flow Inside a Corrugated Enclosure in the Presence of an Inclined Heated Plate*, Prog. Comput. Fluid Dyn. An Int. J., **13**(1), pp. 34-43, 2013.

[39] Al-Amir, Q.R., Alinnawi, F.H.A. & Hamzah, H.K., *Effect of Wavy Wall Location on the Natural Convection in an Enclosure Containing a Concentric Heated Circular Cylinder*, Iraqi J. Mech. Mater. Eng., **17**(2), pp. 291-308, 2017.

[40] Abdulkadhim, A., Hamzah, H.K., Abed, M.A. & Ali, H.F., *Numerical Study of Entropy Generation and Natural Convection Heat Transfer in Trapezoidal Enclosure with a Thin Baffle Attached to Inner Wall Using Liquid Nanofluid*, in Annales de Chimie – Science des Matériaux, **25**(1-2), pp. 7-28, 2017.

[41] Hamzah, H.K., Al-Amir, Q.R., Jabbar, M.Y. & Ali, F.H., Natural Convection Visualization by Heatline for Nanofluids Inside a Square Enclosure Having a Concentric Inner Circular Cylinder at Isoflux Heating Condition on Bottom Wall, J. Eng. Appl. Sci., **13**(14), pp.11006-11023, 2019. DOI: 10.36478/jeasci.2018.11006.11023.

[42] Basak, T. & Chamkha, A.J., *Heatline Analysis on Natural Convection for Nanofluids Confined Within Square Cavities with Various Thermal Boundary Conditions*, Int. J. Heat Mass Transf., **55**(21-22), pp. 5526-5543, 2012.
[43] Bergman, T.L., Incropera, F.P., Dewitt, D.P. & Lavine, A.S., *Fundamentals of Heat and Mass Transfer*, John Wiley & Sons, 2011.